

See discussions, stats, and author profiles for this publication at: <https://www.researchgate.net/publication/280866987>

# Anatase-driven charge transfer involving a spin transition in cobalt iron cyanide nanostructures

ARTICLE *in* PHYSICAL CHEMISTRY CHEMICAL PHYSICS · AUGUST 2015

Impact Factor: 4.49 · DOI: 10.1039/c5cp03580e · Source: PubMed

---

READS

22

## 4 AUTHORS:



**Marco Giorgetti**

University of Bologna

85 PUBLICATIONS 1,269 CITATIONS

SEE PROFILE



**Giuliana Aquilanti**

Sincrotrone Trieste S.C.p.A.

124 PUBLICATIONS 1,201 CITATIONS

SEE PROFILE



**Michela Ciabocco**

University of Bologna

7 PUBLICATIONS 7 CITATIONS

SEE PROFILE

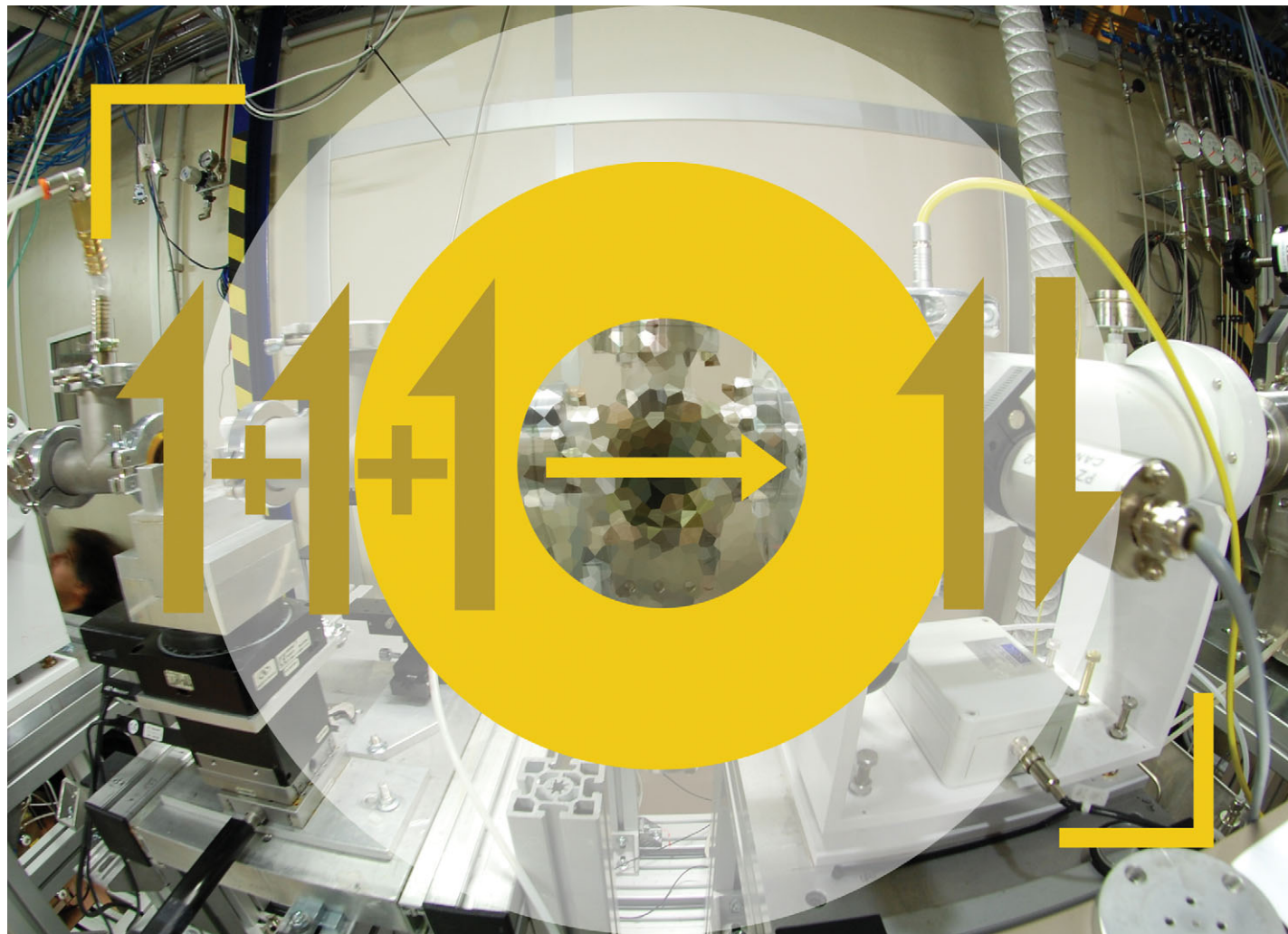


**Mario Berrettoni**

University of Bologna

91 PUBLICATIONS 1,766 CITATIONS

SEE PROFILE

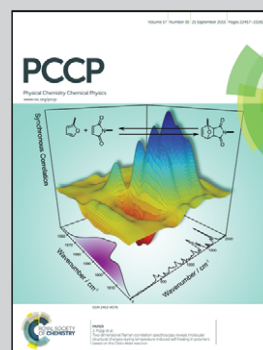


Showcasing research from the laboratory of  
**Prof. Marco Giorgetti at the University of Bologna,  
 Italy and of Dr Giuliana Aquilanti team at  
 Elettra - Sincrotrone Trieste, Italy.**

**Title: Anatase-driven charge transfer involving a spin  
 transition in cobalt iron cyanide nanostructures**

Cobalt hexacyanoferrate can experience a spin transition at the cobalt site. Generally, the difference in the energy of the two spin states is furnished by photoexcitation, as for instance in memory devices and magneto-optical switching applications. The collaborating work done in the two laboratories has led to the evidence of a spin transition at the Co site by an anatase-driven stimulus. The use of the most appropriate X-ray analytical techniques such as high resolution XANES and EXAFS have evidenced, out of the spin transition, a charge transfer accompanied by structural transformation.

### As featured in:



See Marco Giorgetti *et al.*,  
*Phys. Chem. Chem. Phys.*,  
 2015, 17, 22519.



[www.rsc.org/pccp](http://www.rsc.org/pccp)

Registered charity number: 207890

## COMMUNICATION



Cite this: *Phys. Chem. Chem. Phys.*,  
2015, 17, 22519

Received 21st June 2015,  
Accepted 26th July 2015

DOI: 10.1039/c5cp03580e

www.rsc.org/pccp

# Anatase-driven charge transfer involving a spin transition in cobalt iron cyanide nanostructures†

Marco Giorgetti,<sup>a</sup> Giuliana Aquilanti,<sup>b</sup> Michela Ciabocco<sup>c</sup> and Mario Berrettoni<sup>c</sup>

**A charge transfer between Fe and Co in cobalt hexacyanoferrate has been observed for the first time by anatase doping. The charge transfer, which involves a spin transition at the Co site, is supported by high-resolution XANES spectra. EXAFS evidenced a consistent change (10%) of the Co–N first shell.**

Cobalt hexacyanoferrate has long been known<sup>1,2</sup> to undergo a spin transition at the cobalt site. This has been correlated to a charge transfer between the Fe and Co, which induces the Co<sup>II</sup> ( $S = 3/2$ )–Co<sup>III</sup> ( $S = 0$ ) switching, with concomitant structural transformation predominantly attributed to the Co–N bond distance upon the high spin (HS)–low spin (LS) switching. Generally, the difference in the energy of the two spin states is furnished by photoexcitation, and an irradiation energy of 1 eV (red light) is enough to facilitate the spin transition between the two stable states.<sup>3</sup> For instance, a spin transition followed by strong changes in the magnetisation has been observed upon illuminating a cobalt hexacyanoferrate sample with proper light, a fact that has led to applications in memory devices and magneto-optical switching.<sup>4</sup>

Recently, a solid-state magnetic switching mechanism has been proposed *via* proton-coupled electron transfer in cobalt hexacyanoferrate.<sup>5</sup> The renewed attention to this class of polymeric inorganic material is due to their electrocatalytic activity in the water oxidation reaction<sup>6</sup> and in the electrochemical separation of cesium from wastewaters.<sup>7</sup> This paper presents the evidence for a spin transition at the Co site by an anatase-driven stimulus. TiO<sub>2</sub> modifications with transition metals have extended the spectral

response of TiO<sub>2</sub> well into the visible region, also improving its photocatalytic activity.<sup>8–10</sup> The incorporation of transition metals in the titania crystal lattice may result in the formation of new energy levels between VB and CB, inducing a shift of light absorption towards the visible light region. Anatase has proven more efficient than rutile in photocatalysis;<sup>11</sup> hence it is more widely used than rutile in many applications, including the synthesis of supported catalysts, due to its remarkably higher specific surface area.

Samples have been analysed by a joint XANES and EXAFS approach, giving evidence of the local charge changes and local structural modification in TiO<sub>2</sub>-modified samples.

From the structural viewpoint, cobalt hexacyanoferrate materials (Cohcf) of the general formula  $X_aCo_b[Fe(CN)_6]_c \cdot dH_2O$  are NaCl-type with a three-dimensional Fe–C–N–Co network, *Fm3m* (No. 225), where both metals occupy the octahedral 4a Wyckoff position, and water molecules are at the interstitial site. X is an alkali-metal at the 8c site, which guarantees neutrality. The peculiar structure of the material has served for a fundamental study on the four-body multiple scattering contribution in X-ray absorption spectra.<sup>12</sup> Following the ease of Fe–Co charge transfer in cobalt hexacyanoferrates,<sup>13,14</sup> our group also suggested the use of the (FeCo)<sup>ox</sup> number notation for the oxidation state,<sup>15</sup> which represents the actual situation where Co<sup>II/III</sup> and Fe<sup>II/III</sup> metal ions with different ratios can coexist.

Table 1 indicates the investigated samples together with their chemical analysis and XRD data (cell parameter *a* of an *Fm3m* structure).

**Table 1** List of the investigated compounds: stoichiometry and cell parameter *a*

Compounds (formal stoichiometry from chemical analysis)	Cell parameter <i>a</i>	
	From XRD powder, Å (±0.05)	From EXAFS, Å (±0.02)
(I) TiO <sub>2</sub> –K <sub>1.2</sub> Co <sub>1.3</sub> Fe(CN) <sub>6</sub>	10.07	9.86
(II) K <sub>0.4</sub> Co <sub>1.4</sub> Fe(CN) <sub>6</sub>	10.34	10.28
(III) TiO <sub>2</sub> –K <sub>0.6</sub> Fe <sub>1.1</sub> [Co(CN) <sub>6</sub> ]	10.33	10.28
(IV) K <sub>0.5</sub> Fe <sub>1.3</sub> [Co(CN) <sub>6</sub> ]	10.31	10.22

<sup>a</sup> Department of Industrial Chemistry “Toso Montanari”, University of Bologna, Viale Risorgimento 4, 40136 Bologna, Italy. E-mail: marco.giorgetti@unibo.it; Fax: +39 0512093690; Tel: +39 0512093666

<sup>b</sup> Elettra – Sincrotrone Trieste S.C.p.A., s.s. 14 km 163.5, 34149 Basovizza, Trieste, Italy

<sup>c</sup> Dipartimento di Chimica Industriale “Toso Montanari”, UOS, Campus di Rimini, Università di Bologna, Via dei Mille 39, 47921 Rimini, Italy

† Electronic supplementary information (ESI) available: Experimental details, XAS measurements and analysis, contour plots and table of the EXAFS fitting parameters. See DOI: 10.1039/c5cp03580e

The electronic structures of both Fe and Co were first characterized. Fig. 1 displays the X-ray absorption near-edge spectra (XANES) of the four samples at both metal edges (Fe and Co).

All spectra are characterized by a pre-edge peak A, the edge region B corresponding to the rising part of the spectrum, the edge resonance C, which is associated with the continuum, and the region D, which is associated with multiple scattering events of the photo-electron. As seen from the Co K-edge, spectra are modified in both shape and position of the main features, with the largest difference arising from the cobalt hexacyanoferrate when compared to the TiO<sub>2</sub>-doped cobalt hexacyanoferrate sample (blue lines). This difference suggests a strong modification of the local charge associated with the cobalt ion, whereas little modification is seen at the Fe K-edge apart from changes in the local charge associated with Fe, providing evidence for a close interaction between the Co site and the anatase, which in turn may produce changes in the formal oxidation states of the two metals. The same holds true while considering the Fe-K edge spectra, but in this case, the iron hexacyanocobaltate (Fehcc) samples are the ones that show a significant difference. This is related to the structure of the investigated metal hexacyano-metallate: in the hexacyanoferrate, the N-side of the cyanide bridge is linked to the cobalt. On the contrary, the N-side is coordinated by the iron in hexacyanocobaltate. Overall, these findings provide evidence for a close interaction between Ti (of the anatase) and the metal attached to the N-side of the hexacyano-metallate linear chain, which is in line with IR and XPS data.<sup>16</sup>

The local structural sites of both Fe and Co have been analysed using EXAFS. Fig. 2 displays the comparison of the  $k^2$ -extracted EXAFS signals to the theoretical ones for samples **I** and **II** at both Fe and Co edges. The corresponding Fourier transform signals are indicated at the bottom. A similar plot for samples **III** and **IV** are available as ESI.†

The EXAFS curves are characterized by a superposition of several main oscillations, and the corresponding FT curves confirm the presence of three main peaks, which originate by the almost-perfect cube structure of metal hexacyanoferrate.<sup>12</sup> The position of the peaks are not the same in CoHCF and in TiO<sub>2</sub>-doped CoHCF, indicating a modification of the structure upon anatase doping. In particular, at the Co K-edge, all three

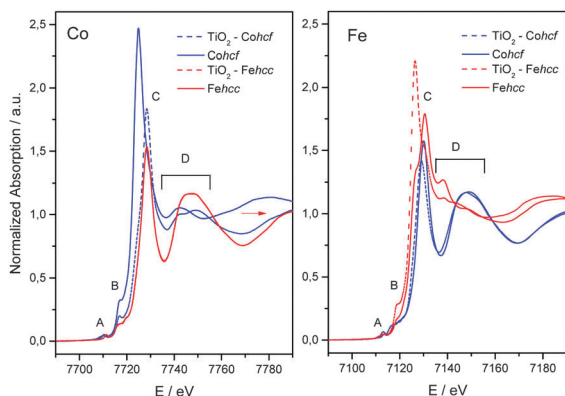


Fig. 1 Normalized XANES spectra at Fe and Co K-edge for all samples.

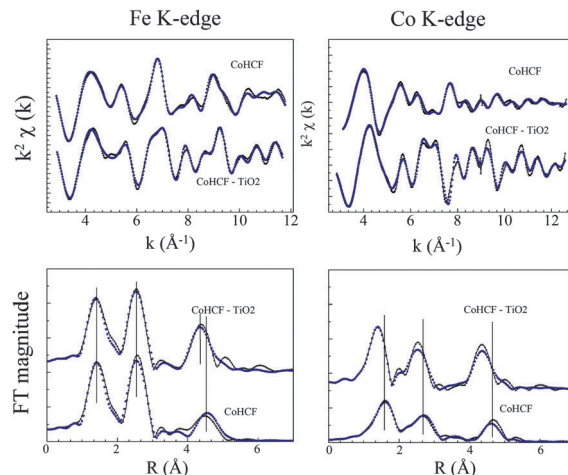


Fig. 2 EXAFS data analysis for samples **I** and **II**. Comparison of the experimental (—) and theoretical (---)  $k^2$ -weighted EXAFS signals (upper panels) and the corresponding Fourier transform (lower panels) of the  $k^2$ -weighted EXAFS for compounds **I** and **II** at Fe and Co K-edges.

peaks shift to lower distances, providing evidence for bond length shortening of the first, second and third shells around the cobalt. This fact is closely correlated to a possible spin transition. On the contrary, at the Fe site, only the 3rd peak at about 5 Å, which corresponds to the Fe–Co mutual distance, is seen to decrease upon TiO<sub>2</sub> doping.

The EXAFS spectrum of metal hcf is a peculiar one, and it requires a specific analysis<sup>12,13,17</sup> concerning the electron scattering from strongly correlated systems, such as the metal hexacyanoferrates. As indicated by the best-fit plot in Fig. 2, the theoretical curves match well within the experimental ones, demonstrating the reliability of the present EXAFS data analysis, which is fully detailed in the ESI.† Table 2 reports some relevant structural parameters (interatomic distances) for all samples as obtained by the best-fitting procedures.

The Fe–C first-shell interatomic distances in samples **I** and **II** are almost the same, with values of 1.892(5) and 1.872(6) Å, respectively. On the contrary, a large difference was found in the Co–N interaction. The observed value of 2.084(5) Å for the pristine CoHcf material shortens to 1.891(7) Å in the TiO<sub>2</sub>-doped sample. This significant difference is found to be correlated to a spin transition from Co high spin ( $S = 3/2$ ) to Co low spin ( $S = 0$ ), which is accompanied by a variation of the Co–N bond length, as observed previously.<sup>18,19</sup> In this case, a partial electron transfer from Co<sup>II</sup>-LS to Fe<sup>III</sup> should be observed, which in turn triggers the formation

Table 2 Selected structural parameters from EXAFS fitting results of samples **I–II** (cobalt hexacyanoferrate) and **III–IV** (iron hexacyanocobaltate). The estimated parameter errors are indicated in parentheses

Interatomic distances	<b>I</b>	<b>II</b>	<b>III</b>	<b>IV</b>
Fe–C/Å	1.872(6)	1.892(5)	—	—
Co–C/Å	—	—	1.868(2)	1.859(4)
C≡N/Å	1.171(5)	1.166(5)	1.19(1)	1.19(1)
Co–N/Å	1.891(7)	2.084(5)	—	—
Fe–N/Å	—	—	2.087(3)	2.061(4)



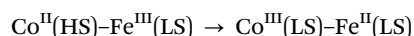
of  $\text{Co}^{\text{III}}$ -LS. This spin transition is not observed in samples **III** and **IV**, *i.e.*, while the hexacyanocobaltate of  $\text{Fe}(\text{II})$  is doped with  $\text{TiO}_2$ . In such a case, the first-shell distance at both Fe and Co does not change significantly upon doping the pristine material.

The  $\text{C}\equiv\text{N}$  bond lengths, ranging from 1.166(5) to 1.19(1) Å in all four samples, are comparable to the values quoted for this class of materials.<sup>12,13</sup> The EXAFS Debye Waller generally increases in several structural parameters after  $\text{TiO}_2$  doping, demonstrating an increase of the structural disorder. This is evident from a comparison of the EXAFS bond variance associated with the first-shell Fe–C and Co–C distances. It is also interesting to note that the errors associated with the structural parameters, as indicated in the Table 2, are in line with those of similar samples in bulk and film.<sup>12,13,17</sup> The errors have been determined by the correlation maps (contour plot) for each pair of highly correlated parameters. Examples of contour plots are reported in the ESI† (Fig. S2). Overall, the EXAFS analysis indicates a consistent shortening (about 10%) of the Co–N bond length in the Cohcf sample upon  $\text{TiO}_2$  addition and that the Fe–C–N portion of the Fe–C–N–Co linear chains vibrate in the same way around the equilibrium position. Also,  $\text{TiO}_2$  doping triggers some structural disorder in both Cohcf and Fehcc.

Detailed electronic information can be gained by the analysis of the pre-edge peaks and of both Fe and Co K-edge XAS spectra. To this end, high-resolution XANES spectra have been recorded at the same beamline but using a pair of Si(311) crystals in the fixed-exit monochromator, ensuring better experimental resolution. Fig. 3 shows the pre-edge side of the XANES spectra at both the Co (left) and Fe (right) K-edge. Generally speaking, pre-edge peaks of first-row transition metals are due to the dipole-forbidden  $1s\text{--}3d$  transition, which becomes possible by  $p\text{--}d$  hybridisation if distortion from centrosymmetry takes place.<sup>20</sup> In our case, because both Co and Fe are in almost-perfect octahedral symmetry, those weak pre-edge peaks are due most likely to quadrupole-allowed  $1s\text{--}3d$  transition.<sup>20</sup> The Co pre-edge features are mainly characterized by a single peak, with different intensities and positions in the studied samples. In the pristine Cohcf ( $\text{Co}^{\text{II}}\text{--HS}$ ), the peak moves towards higher energy, and thus an oxidation (to  $\text{Co}^{\text{III}}\text{--LS}$ ) takes place. On the contrary, no changes in the edge energy nor the intensity are observed in the  $\text{TiO}_2$ -modified

Fehcc sample: the Co oxidation state remains unchanged. It is also interesting to note the shift in the peak position (about 1 eV) observed for  $\text{Co}^{\text{III}}$  coordinated by 6C (as in the Fehcc sample) with respect to the 6 N-coordinated  $\text{Co}^{\text{III}}$  sample ( $\text{TiO}_2\text{--Cohcf}$  sample). This shift is due to a crystal field effect: the C-bonded cyanide ligand produces a larger crystal field than the N-bonded one, and thus the peaks move towards higher energy.

The pre-edge features at the Fe K-edge are more complicated, but a close inspection provides clear evidence of the reduction of  $\text{Fe}^{\text{III}}$  to  $\text{Fe}^{\text{II}}$  in the  $\text{TiO}_2$ -modified Cohcf sample, with respect to the pristine. This allows us to explore the possible charge transfer among the two metals: an oxidation of  $\text{Co}^{\text{II}}$  and a reduction of  $\text{Fe}^{\text{III}}$  have been evidenced. Overall, this result well correlates to the outcome of the EXAFS data analysis. In fact, anatase doping of the Cohcf sample caused a major shortening of the Co–N bond length, which is a well-known experimental finding correlated to a Co spin transition.<sup>14,15</sup>  $\text{TiO}_2$  induces an electronic charge transfer concomitant to a significant shortening of the Co–N bond length from 2.08 Å ( $\text{Co}^{\text{II}}\text{--HS}$ ) to 1.91 Å ( $\text{Co}^{\text{III}}\text{--LS}$ ) and with a subsequent shortening of the cell parameters from 10.28 to 9.96 Å (as indicated in Table 2). Overall, the charge transfer involving the spin transition in Cohcf can be indicated as:



Samples **III** and **IV** (Fehcc and  $\text{TiO}_2$ -modified Fehcc, red lines) are subject to changes related to symmetry at the Fe site, but none at the Co site. This is also evidenced by the pre-edge curves. More information at the Fe site can be deduced by the high-resolution spectra, which allowed the identification of three peaks (A1, A2 and A3), which are expected for high-spin (HS) ferrous complexes. Even though the multiplex analysis of the pre-edge spectra at the Fe K-edge are outside the aim of the present work (a full reference can be found in ref. 16), the three peaks are due to the  $1s\text{--}3d_{t_{2g}}$  ( $^4\text{T}_{1g}$ ) and to the  $1s\text{--}3d_{e_g}$  ( $^4\text{T}_{2g}$  and  $^4\text{T}_{1g}$ ) states. The energies of the three peaks A1, A2 and A3 are very close to those of the  $\text{Fe}(\text{II})$ imidazole,<sup>20</sup> a six-fold, N-coordinated  $\text{Fe}(\text{II})$  complex. Eventually, the pre-edge data at the Fe K-edge support the LS state of iron for samples **I** and **II** (6C coordinated) and the HS state for samples **III** and **IV** (6N coordinated).

In conclusion, a charge transfer in anatase-doped cobalt hexacyanoferrate has been proven. The experimental evidence is supported by high-resolution XANES and EXAFS spectroscopy, the latter also indicating a consistent change (10%) of the Co–N first-shell bond distance, which in turn causes an equivalent variation of the cell parameter *a* of the lattice. The spin transition has not been observed in the analogous compound where the Fe and Co ions are swept. This is most likely due to a difference in the energy for the spin transition to occur in the two materials. To our knowledge, this represents one of the first examples where an external stimulus other than photoexcitation triggers spin-crossover phenomena in a metal hexacyanoferrate-based molecular solid. We have also seen that the ligand field plays an important role, as the pre-edge data at the Fe K-edge support the LS state of iron for samples **I** and **II** (6C coordinated) and the HS state for samples **III** and **IV** (6N coordinated).

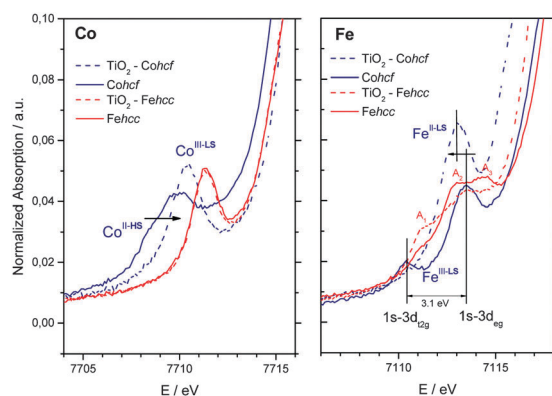


Fig. 3 Pre-edge data for samples **I–IV** recorded using a pair of Si(311) crystals, at the Fe and Co K-edge.

Samples were prepared by following the method by Berrettoni *et al.*<sup>16</sup> X-ray absorption measurements were recorded at the XAFS beamline at Elettra Synchrotron (Basovizza, Trieste, Italy). The storage ring was operated at 2.0 GeV in top-up mode with a typical current of 300 mA. The data were recorded at Fe K-edge (7112 eV) and Co K-edge (7709 eV) in transmission mode using the ionization chamber. Full details on the experimental procedures are available as ESI.†

XAS experiments at ELETTRA Sincrotrone Trieste were supported by proposal #20125309.

## Notes and references

- 1 O. Sato, T. Iyoda, A. Fujishima and K. Hashimoto, *Science*, 1996, **272**, 704.
- 2 A. Bleuzen, C. Lomenech, V. Escax, F. Villain, F. Varret, C. Cartier Dit Moulin and M. Verdager, *J. Am. Chem. Soc.*, 2000, **122**, 6648.
- 3 Y. Ogawa, S. Koshihara, K. Koshino, T. Ogawa, C. Urano and H. Tagaki, *Phys. Rev. Lett.*, 2000, **84**, 3181.
- 4 T. Matsuda, H. Tokoro, K. Hashimoto and S. I. Ohkoshi, *Dalton Trans.*, 2006, 5046.
- 5 P. Higel, F. Villain, M. Verdager, E. Rivière and A. Bleuzen, *J. Am. Chem. Soc.*, 2015, **136**, 6231.
- 6 S. Pintado, S. Goberna-Ferron, E. C. Escudero-Adan and J. R. Galan-Mascaros, *J. Am. Chem. Soc.*, 2013, **135**, 13270.
- 7 R. Chen, H. Tanaka, T. Kawamoto, M. Asai, C. Fukushima, M. Kurihara, M. Ishisaki, M. Watanabe, M. Arisaka and T. Nankawa, *ACS Appl. Mater. Interfaces*, 2013, **5**, 12984.
- 8 M. Pelaez, N. T. Nolan, S. C. Pillai, M. K. Seery, P. Falaras, A. Kontos, P. S. M. Dunlop, J. W. J. Hamilton, J. A. Byrne, K. O'Shea, M. H. Entezari and D. D. Dionysiou, *Appl. Catal., B*, 2012, **125**, 331.
- 9 M. Berrettoni, M. Ciabocco, M. Fantauzzi, M. Giorgetti, A. Rossi and E. Caponetti, *RSC Adv.*, 2015, **5**, 35435.
- 10 A. Fujishima, T. N. Rao and D. A. Tryk, *J. Photochem. Photobiol., C*, 2010, **1**, 1.
- 11 X. Wang, A. Kafizas, X. Li, S. J. A. Moniz, P. J. T. Reardon, J. Tang, I. P. Parkin and J. R. Durrant, *J. Phys. Chem. C*, 2015, **119**, 10439.
- 12 M. Giorgetti, M. Berrettoni, A. Filipponi, P. J. Kulesza and R. Marassi, *Chem. Phys. Lett.*, 1997, **275**, 108.
- 13 M. Giorgetti, L. Guadagnini, D. Tonelli, M. Minicucci and G. Aquilanti, *Phys. Chem. Chem. Phys.*, 2012, **14**, 5527.
- 14 M. Giorgetti, M. Berrettoni, S. Zamponi, P. J. Kulesza and J. A. Cox, *Electrochim. Acta*, 2005, **51**, 511.
- 15 M. Berrettoni, M. Giorgetti, S. Zamponi, P. Conti, D. Ranganathan, A. Zanolto, M. L. Saladino and E. Caponetti, *J. Phys. Chem. C*, 2010, **114**, 6401.
- 16 M. Berrettoni, M. Ciabocco, M. Fantauzzi, M. Giorgetti, A. Rossi and E. Caponetti, *RSC Adv.*, 2015, **5**, 35435.
- 17 M. Giorgetti and M. Berrettoni, *Inorg. Chem.*, 2008, **47**, 6001.
- 18 T. Yokohama, T. Otha, O. Sato and K. Hashimoto, *Phys. Rev. B: Condens. Matter Mater. Phys.*, 1998, **58**, 8257.
- 19 V. Escax, G. Champion, M. A. Arrio, M. Zacchigna, C. Cartier Dit Moulin and A. Bleuzen, *Angew. Chem., Int. Ed.*, 2005, **44**, 4798.
- 20 T. E. Westre, P. Kennepohl, J. G. DeWitt, B. Hedman, K. O. Hodgson and E. I. Solomon, *J. Am. Chem. Soc.*, 1997, **119**, 6297.